Berberine ameliorates CCl$_4$-induced liver injury in rats through regulation of the Nrf2-Keap1-ARE and p53 signaling pathways

CHUN-YANG HAN[1*], TAO-TAO SUN[1*], GUANG-PEI XV[1*], SI-SI WANG[1], JIN-GANG GU[2] and CUI-YAN LIU[1]

[1]College of Animal Science and Technology, Anhui Agricultural University, Hefei,
Anhui 230036; [2]Institute of Agricultural Resources and Regional Planning,
Chinese Academy of Agricultural Sciences, Beijing 100081, P.R. China

Abstract. Berberine (BBR) is an isoquinoline alkaloid, reported to have multiple pharmacological functions. However, its effects against CCl$_4$-induced oxidative damage remain poorly studied. Therefore, the present study investigated the protective action of BBR, and its antioxidant mechanisms, against CCl$_4$-induced liver injury in rats. A total of 48 rats were randomly arranged into six groups: Control; model; positive control (PC); BBR low-dose (BL); BBR middle-dose (BM); and BBR high-dose (BH). The BL, BM and BH animals received BBR (5, 10 and 15 mg/kg by weight, respectively) orally for 7 consecutive days. Rats in the PC group were given silymarin (150 mg/kg), and the control and model groups were administered distilled water orally. At the end of the experiment, blood samples and livers were collected. To measure the liver biochemical indices, the reactive oxygen species (ROS) generation and the expression levels of related genes and protein, the following methods were used: An automatic biochemical analyzer; flow cytometry; spectrophotometry; reverse transcription-quantitative PCR; western blotting; and hematoxylin and eosin staining. The results revealed that BBR significantly decreased the serum levels of alanine transaminase, aspartate transaminase and alkaline phosphatase, and increased those of glutathione and superoxide dismutase, but decreased malondialdehyde activity in hepatic tissue, and significantly decreased the reactive oxygen species level in hepatocytes. In hepatic tissue, the expressions of nuclear factor erythroid 2-related factor 2 (Nrf2), kelch-like ECH-associated protein 1 (Keap-1), NAD(P)H quinone dehydrogenase 1 (*NQO-1*), heme oxygenase 1 (*HO-1*), *Bcl-2* and *Bcl-xL* mRNA, and HO-1 protein were elevated, and the expression of *p53* mRNA was decreased, particularly in the BH group (15 mg/kg). In conclusion, BBR exerts a protective action against CCl$_4$-induced acute liver injury in rats via effectively regulating the expression of Nrf2-Keap1-antioxidant responsive element-related genes and proteins, and inhibiting p53 pathway-mediated hepatocyte apoptosis.

Introduction

Acute liver injury (ALI) is a disease caused by drug poisoning, viral infection, immune reactions or vascular disorders, resulting in acute abnormal liver function. The clinical manifestation is acute hepatic dysfunction. ALI can subsequently develop into acute liver failure, which is characterized by rapidly progressing hepatic encephalopathy and multiple organ failure, with a poor prognosis and high mortality rate (1). To date, no effective treatment for ALI has been found. Berberine (BBR) is an isoquinoline alkaloid found in plants of the families Berberidaceae, Papaveraceae, Ranunculaceae, Rutaceae and Physalis (Fig. 1) (2). Studies have shown that BBR has many pharmacological functions, as well as antibacterial, anti-inflammatory, anti-tumor, cardioprotective and hypoglycemic properties; it also regulates lipid metabolism and immunosuppression, and protects the central nervous system (3-6). A previous study by the authors found that 0.004 mg/ml BBR exerts a protective function against lipopolysaccharide-induced inflammatory injury to hepatocytes in rats, but doses >0.005 mg/ml can increase reactive oxygen species (ROS) levels in L929 cells (7). In the current study, to further explore the effects of BBR on liver damage, CCl$_4$-induced ALI in rats was used as a pathological model, and BBR was used as an interventional therapy. Before and after the treatment, the macroscopic, biochemical and histological changes in the liver were observed. The mRNA expression levels of nuclear factor erythroid 2-related factor 2 (Nrf2)-kelch-like ECH-associated protein 1 (Keap1)-antioxidant responsive element (ARE) signaling pathway-related genes [*Nrf2*, *Keap-1*, NAD(P)H quinone dehydrogenase 1 (*NQO-1*) and heme oxygenase 1 (*HO-1*)], p53 signaling pathway-related genes (*p53*, *Bcl-2* and *Bcl-xL*),

Correspondence to: Dr Cui-Yan Liu, College of Animal Science and Technology, Anhui Agricultural University, 130 West Changjiang Road, Hefei, Anhui 230036, P.R. China
E-mail: cyliu@ahau.edu.cn

[*]Contributed equally

and HO-1 protein expression, were detected. The results obtained may provide an experimental basis for the clinical use of BBR in the treatment of liver injury.

Materials and methods

Chemicals. BBR (Sigma-Aldrich; Merck KGaA), BBR standard (Dalian Meilun Biotech Co., Ltd.), silymarin (Shanghai Yuanye Biotechnology Co., Ltd.), CCl$_4$ (Xilong Chemical Co., Ltd.), detection kits for ROS, total superoxide dismutase (T-SOD), catalase (CAT), malondialdehyde (MDA), glutathione (GSH), aspartate transaminase (AST), alanine transaminase (ALT) and alkaline phosphatase (ALP) (all from Nanjing Jiancheng Bioengineering Institute), RNA extract (Google Biotechnology Co., Ltd., Wuhan, China), alcohol, isopropanol and trichloromethane (all from Sinopharm Chemical Reagent Co., Ltd.) were purchased from the suppliers indicated. HyPure™ molecular biology grade water was purchased from HyClone; GE Healthcare Life Sciences. The RevertAid First Strand cDNA Synthesis kit was procured from Thermo Fisher Scientific, Inc. FastStart Universal SYBR Green Master (Rox) was supplied by Roche Diagnostics. Primers were synthesized by Sangon Biotech Co., Ltd.

Animals. In total, 48 5-week-old male Sprague-Dawley (SD) rats (180-200 g) were obtained from Guangzhou TianCheng Medical Technology Co., Ltd. [animal license no. SCXK (Su) 2014-0007]. The animals were maintained in standard housing facilities (24±1˚C; 45±5% relative humidity; 12-h light/dark cycle), and fed a standard laboratory diet, with *ad libitum* access to water. All animals were given a week to acclimatize before the experiment. All procedures were in strict accordance with the Chinese legislation on the use and care of laboratory animals and the guidelines established by the Institute for Experimental Animals of Anhui Agriculture University, and were approved by the Anhui Agriculture University Committee on Animal Care and Use.

Animal grouping and treatment. The 48 SD rats were randomly divided into six groups (n=8): Control; model; positive control (PC); BBR low-dose (BL); BBR middle-dose (BM); and BBR high-dose (BH). The rats of the BC, BM and BH groups received BBR (5, 10 and 15 mg/kg body weight, respectively) orally for 7 consecutive days. The positive control (PC) group animals were given silymarin (150 mg/kg). The control and model animals were administered distilled water orally for 7 days. A total of 6 h after the last gavage, the model, PC, BL, BM and BH rats were given 50% CCl$_4$ oil solution (1 ml/kg, intraperitoneally), and the control rats were given the same amount of soybean oil solvent. At 24 h after the injection, the rats were weighed and sacrificed. Blood samples from the heart (3-5 ml) and livers were collected and a liver autopsy was conducted, followed by several other laboratory tests, as described below.

Pathological examination. The size, color, smoothness, hardness and elasticity of the liver were visually observed, and common pathological changes, such as swelling, nodules, necrosis, degeneration, hemorrhage and congestion, were noted.

Biochemical indices of the liver (AST and ALT). Non-anticoagulant samples were centrifuged at 4˚C, 1,106 x g for 5 min to separate the serum. Serum levels of AST and ALT were detected using an automatic biochemistry analyzer (Catalyst Dx; IDEXX Laboratories, Inc.).

Detection of the ROS level in hepatocytes. The fresh liver was cut into several 1 mm^3 pieces using ophthalmic scissors, digested using trypsin, and filtered to obtain a single-cell suspension. The ROS level was detected by flow cytometry (FACSCalibur; Becton, Dickinson and Company), according to the instructions supplied with the ROS test kit. CellQuest version 6.0 (Becton, Dickinson and Company) was used for the collection and analysis of data.

Detection of biochemical indices in liver tissue. A portion of the liver was taken and homogenized using a tissue homogenizer (KZ-II; Servicebio) to obtain a 10% tissue homogenate, which was centrifuged for 10 min at 1,106 x g at 4˚C and the supernatant collected. Levels of T-SOD, MDA, and GSH were spectrophotometrically detected (Pharo 300; Merck KGaA).

Detection of HO-1 protein expression in hepatic tissues by western blotting. Total proteins were extracted after cell lysis using RIPA buffer (Servicebio), for western blotting and immunoprecipitation with PMSF. Proteins were quantified using the bicinchoninic acid assay. Equal amounts of protein were loaded onto a 12% SDS-PAGE gel, electrophoresed, transferred to a nitrocellulose membrane, and blocked with 5% skim milk for 1 h at room temperature. The membrane was incubated with primary antibodies against anti-HO-1 (1:1,000; cat no. 10701-1-AP; Wuhan Sanying Biotechnology) and GAPDH (1:1,000; cat. no. GB12002; Servicebio) at 4˚C overnight and then washed with TBS with Tween-20, followed by incubation with a peroxidase-labeled secondary antibody for 30 min at room temperature (1:3,000; cat. no. GB23303; Servicebio). Protein visualization was achieved using enhanced chemiluminescence western blotting reagents (Servicebio) and the multi-spectral imaging system (VersaDoc™ 4000 MP; Bio-Rad Laboratories, Inc.).

Detection of the expression of Nrf2, Keap-1, NQO-1, HO-1, P53, Bcl-2 and Bcl-xL mRNA by reverse transcription-quantitative PCR(RT-qPCR). Liver tissues were stored at -80˚C. Liver samples were ground with liquid nitrogen, and the total liver RNA was extracted with TRIzol® reagent (Thermo Fisher Scientific, Inc.) and then reverse-transcribed to cDNA, according to the manufacturer's instructions. Samples were then amplified using qPCR, as specified in the instructions supplied with the FastStart Universal SYBR Green Master (Rox) kit. PCR conditions were as follows: 95˚C for 10 min, 40 cycles of 95˚C for 15 sec and 60˚C for 1 min, and 95˚C for 15 sec. The relative mRNA expression of target genes compared to GAPDH was calculated using the $2^{-\Delta\Delta Cq}$ method (8).

Histopathological examinations. Rat liver tissues were fixed in a 4% buffered formalin solution for 7 days at room temperature and dehydrated using a standard alcohol-xylol process (75, 85, 95 and 100% alcohol, alcohol:xylene=1:1, xylene), embedded in paraffin, cut into 5-μm-thick sections using
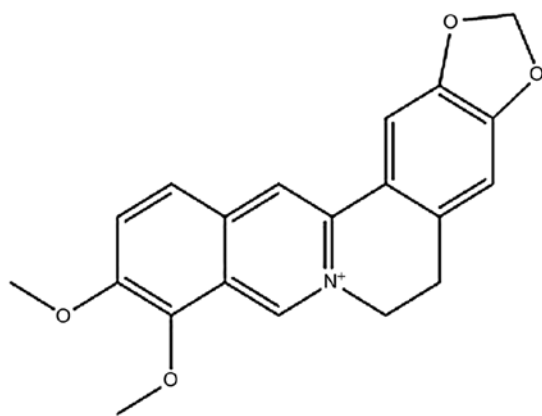
Figure 1. Molecular structure of berberine.

an LS-2055+ paraffin semiautomatic machine (Shenyang LongShou Electronic Instrument Co., Ltd), and stained with hematoxylin and eosin at room temperature as follows: xylene I, 10 min; xylene II, 10 min; 100% alcohol I, 2 min; 100% alcohol II, 2 min; 95% alcohol I, 2 min; 95% alcohol II, 2 min; 85% alcohol, 2 min; hematoxylin, 30 sec; color separation solution, 3 sec; anti-blue solution, 10 sec; eosin, 10 sec; 85% alcohol, 2 min; 95% alcohol II, 2 min; 95% alcohol I, 2 min; 100% alcohol II, 2 min; 100% alcohol I, 2 min; xylene II, 2 min; and xylene I, 2 min. Liver sections were examined by light microscopy using a biological microscope (magnification, x400; CX21FS1; Olympus Corporation).

Statistical analysis. Data were analyzed using IBM SPSS 19.0 (IBM Corp.), and the results expressed as the mean ± SEM. One-way analysis of variance was used to compare the groups, followed by Duncan's test. $P < 0.05$ was considered to indicate a statistically significant difference.

Results

Liver pathological changes. The livers of the control group were reddish-brown, with a smooth surface, neat edge and uniform thickness. The livers of the model group were yellowish-brown and overtly swollen, with necrotic spots on the surface and a rounded edge. The histopathological lesions were effectively attenuated in the drug-treated groups, to varying extents, and the livers of the BM, BH and PC groups had the least swelling, while necrotic spots on the surface were markedly reduced.

Levels of serum ALT, AST and ALP. Compared with the control group, serum ALT, AST, and ALP levels in the model group were increased ($P < 0.05$). Rats of the BBR-treated and PC groups exhibited a decrease ($P < 0.05$) in serum ALT, AST and ALP levels when compared with the model group; these differences were more evident in the BH group than in the BL, BM and PC groups (Fig. 2).

Levels of GSH, T-SOD and MDA in hepatic tissues. Compared with the control group, GSH and T-SOD levels in hepatic tissues in the model group were decreased ($P < 0.05$) and the MDA content was increased ($P < 0.05$). Compared with the model group, liver GSH levels in the BM and BH groups were increased ($P < 0.05$), whereas there were no significant ($P > 0.05$) difference between the model and BL groups. T-SOD levels in the BBR-treated groups were comparable ($P > 0.05$) to those in the model rats, but the liver MDA level in the BH and PC groups was significantly ($P < 0.05$) decreased (Fig. 3).

Level of ROS in hepatocytes. Compared with the control group, the liver ROS level of the model group was increased ($P < 0.05$). Rats of the BBR-treated and PC groups exhibited a significant ($P < 0.05$) decrease in the ROS level in hepatocytes when compared with the model group. The ROS level of the BH group was similar to that of the control group ($P > 0.05$; Fig. 4).

Levels of Nrf2, Keap-1, NQO-1 and HO-1 mRNA in hepatic tissue. Compared with the control group, the liver *Nrf2* mRNA level of the model group was decreased ($P < 0.05$). Compared with the model group, BL, BM and PC rats showed upregulation of *Nrf2* mRNA expression ($P > 0.05$), but only BH rats exhibited a significant upregulation ($P < 0.05$) of *Nrf2* mRNA expression. Although the expression of *Keap-1* mRNA in rat hepatic tissues in the model group was increased, it was not significantly different ($P > 0.05$) from that in the control group. BBR upregulated ($P < 0.05$) the expression of *Keap-1* mRNA in comparison to the model group. The expression of *HO-1* mRNA in rat hepatic tissues in the model group was decreased, but the difference was not significant ($P > 0.05$) compared with the control group. A low dose of BBR slightly upregulated the expression of *HO-1* mRNA ($P > 0.05$), and middle or high doses of BBR significantly ($P < 0.05$) upregulated the expression of *HO-1* mRNA. Rats of the model group exhibited a decrease ($P < 0.05$) in the *NQO-1* mRNA level in hepatic tissues when compared with the control group. In comparison to the model group, BBR upregulated ($P < 0.05$) the expression of *NQO-1* mRNA in the rat hepatic tissue, and silymarin slightly upregulated ($P > 0.05$) the expression of *NQO-1* mRNA (Fig. 5).

Levels of p53, Bcl-2, and Bcl-xL mRNA in hepatic tissues. The expression of *p53* mRNA was increased ($P < 0.05$) in the hepatic tissue of the model group compared with the control group. The expression of *p53* mRNA in the hepatic tissue in the BBR-treated groups and the silymarin group was decreased ($P < 0.05$) compared with the model group. The expression of *Bcl-2* mRNA was lower ($P < 0.05$) in the model group than the control group, whereas those in the low-dose BBR group and the silymarin group were higher ($P < 0.05$) than that in the model group while there was no significant ($P > 0.05$) difference between the medium- and high-dose BBR groups and the model group. In comparison to the control group, the expression of *Bcl-xL* mRNA was somewhat decreased ($P > 0.05$) in the liver tissue of the model group while those in the low-, medium-and high-dose BBR groups, and the silymarin group, were increased ($P < 0.05$; Fig. 6).

Effects of BBR on liver histopathology. The control group livers presented with normal architecture of the hepatocytes and intact cytoplasm. The structure of the hepatic lobule was clear, and the hepatic cord was arranged radially. The nucleus
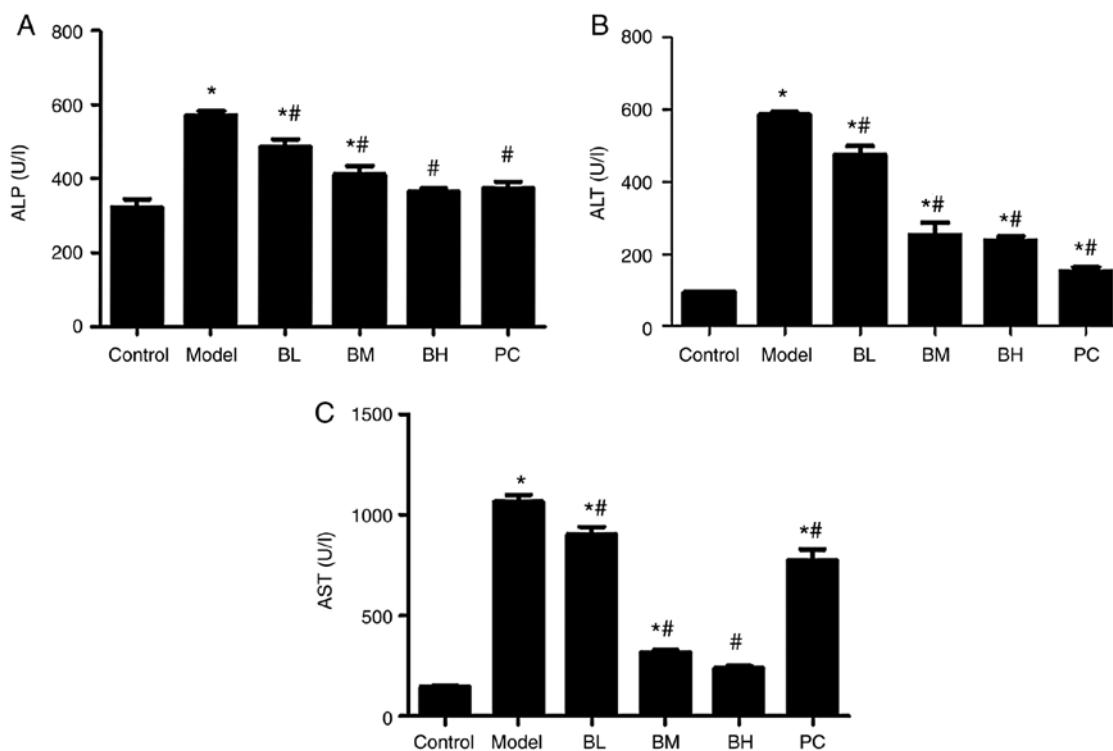
Figure 2. Levels of serum ALP, ALT and AST in the different groups. (A) Levels of serum ALP in the different groups. (B) Levels of serum ALT in the different groups. (C) Levels of serum AST in the different groups. n=8 per group. *P<0.05 vs. control; #P<0.05 vs. model. ALP, alkaline phosphatase; ALT, alanine transaminase; AST, aspartate transaminase; BL, berberine low-dose; BM, berberine middle-dose; BH, berberine high-dose; PC, positive control.
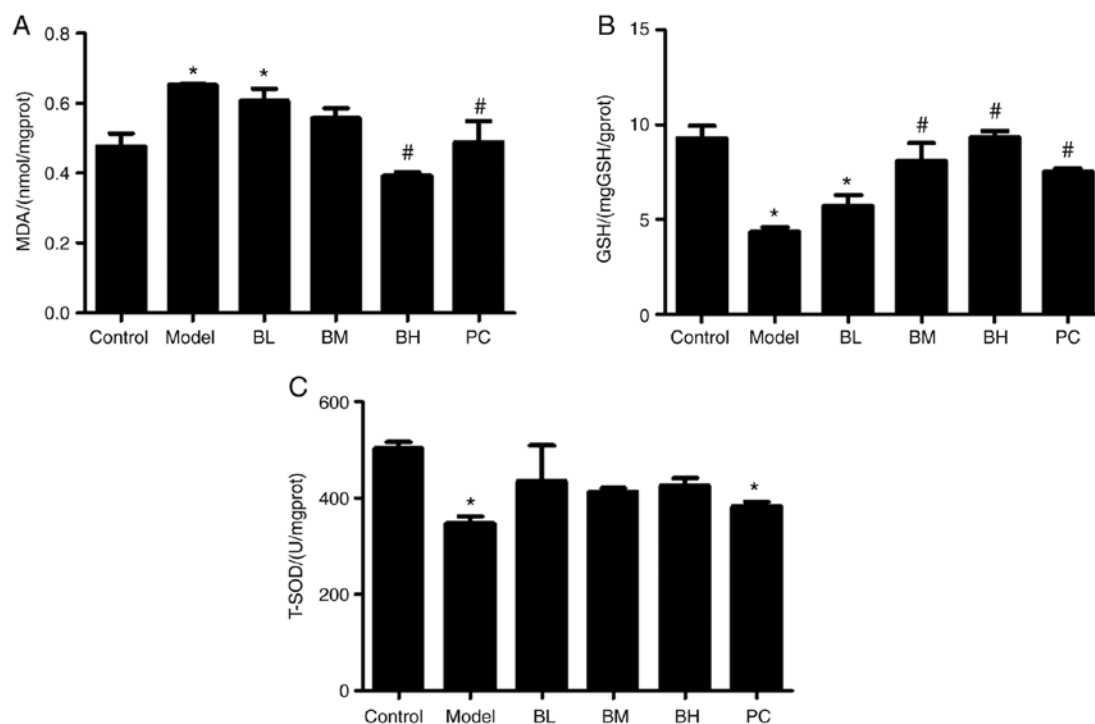

Figure 3. Levels of MDA, GSH and T-SOD in hepatic tissues from the different groups. (A) Levels of MDA in hepatic tissues from the different groups. (B) Levels of GSH in hepatic tissues from the different groups. (C) Levels of T-SOD in hepatic tissues from the different groups. n=8 per group. *P<0.05 vs. control; #P<0.05 vs. model. MDA, malondialdehyde; GSH, glutathione; T-SOD, total superoxide dismutase; BL, berberine low-dose; BM, berberine middle-dose; BH, berberine high-dose; PC, positive control.

of the hepatocyte was centrally located. The hepatocytes in the model group showed an irregular arrangement, as well as

cellular edema and necrosis. The cytoplasmic vacuolization of hepatocytes was noticeable. Hepatocyte edema was reduced in
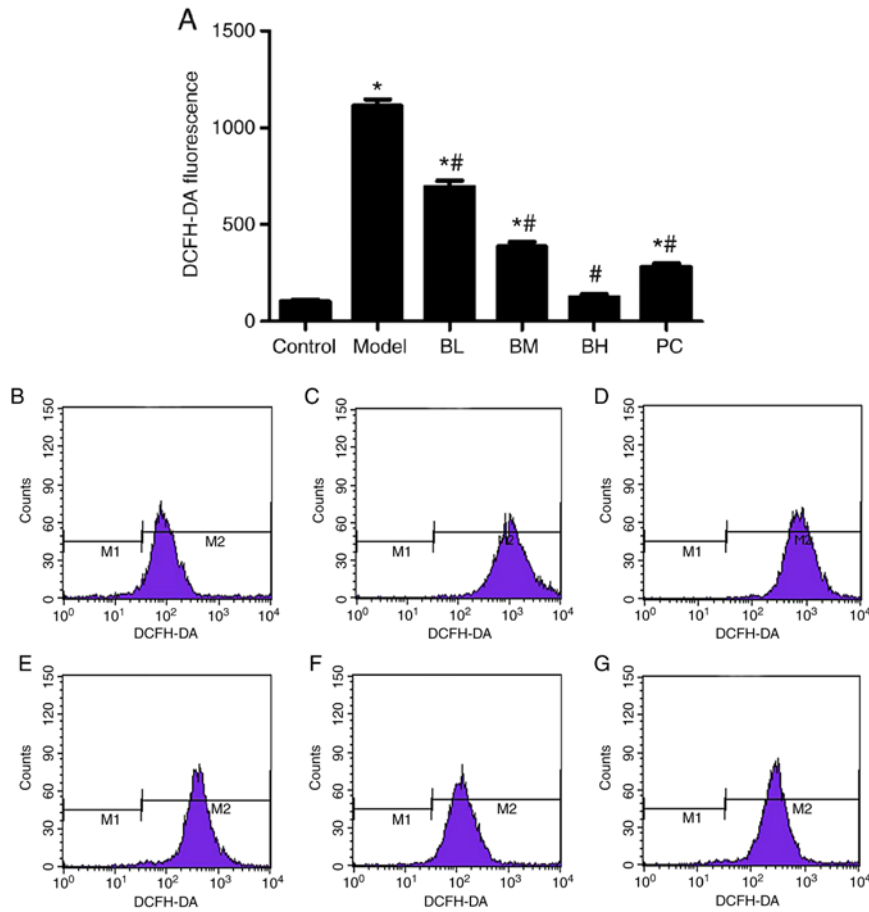
Figure 4. Levels of ROS in hepatocytes from the different groups. (A) Levels of ROS in hepatocytes from the different groups. (B) Levels of ROS in hepatocytes of the control group. (C) Levels of ROS in hepatocytes of the model group. (D) Levels of ROS in hepatocytes of the BL group. (E) Levels of ROS in hepatocytes of the BM. (F) Levels of ROS in hepatocytes of the BH group. (G) Levels of ROS in hepatocytes of the PC group. n=8 per group. $^{*}P<0.05$ vs. control; $^{\#}P<0.05$ vs. model. BL, berberine low-dose; BM, berberine middle-dose; BH, berberine high-dose; PC, positive control; ROS, reactive oxygen species; DCFH-DA, 2',7'-dichlorodihydrofluorescein diacetate.
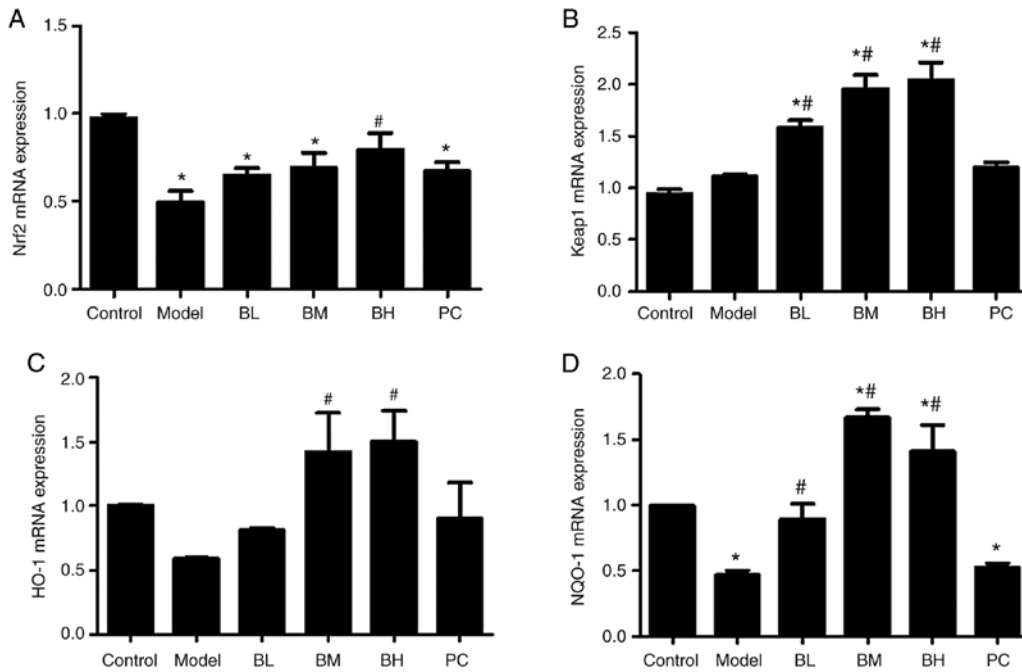

Figure 5. Levels of *Nrf2, Keap-1, HO-1* and *NQO-1* mRNA in hepatic tissues. (A) Level of *Nrf2* mRNA in hepatic tissues. (B) Level of *Keap-1* mRNA in hepatic tissues. (C) Level of *HO-1* mRNA in hepatic tissues. (D) Level of *NQO-1* mRNA in hepatic tissues. n=8 per group. $^{*}P<0.05$ vs. control; $^{\#}P<0.05$ vs. model. BL, berberine low-dose; BM, berberine middle-dose; BH, berberine high-dose; *PC*, positive control; Nrf2, nuclear factor erythroid 2-related factor 2; Keap-1, kelch-like ECH-associated protein 1; HO-1, heme oxygenase 1; NQO-1, NAD(P)H quinone dehydrogenase 1.
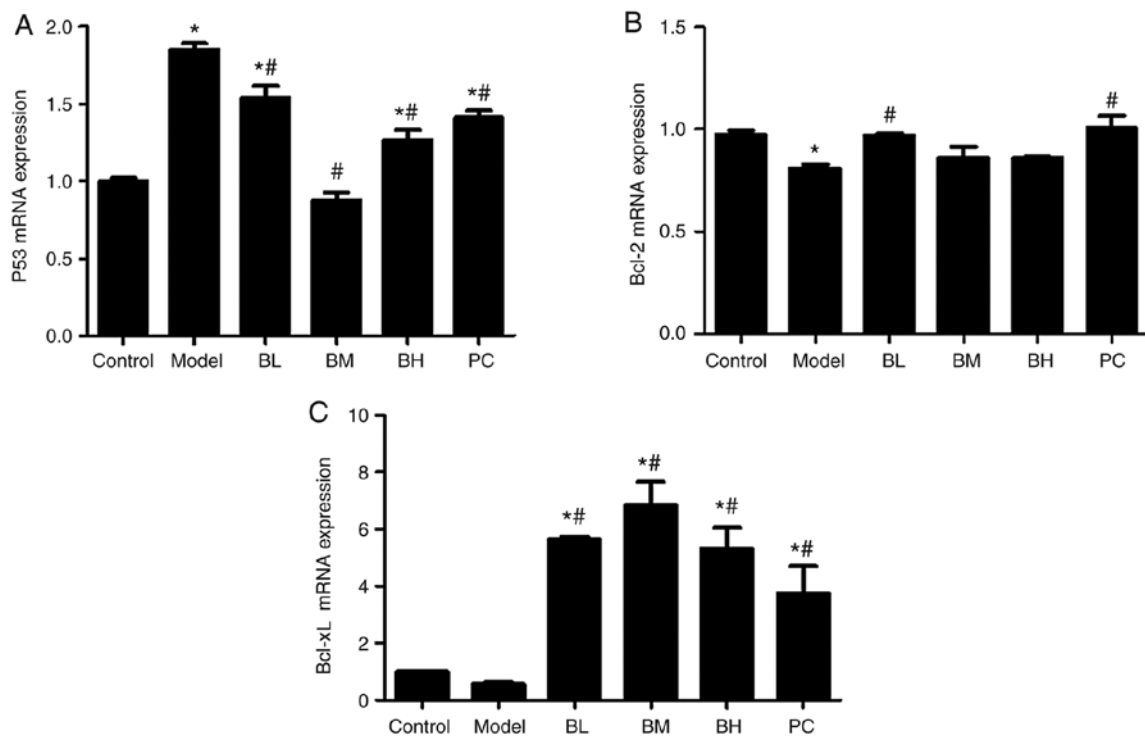
Figure 6. Level of *p53*, *Bcl-2* and *Bcl-xL* mRNA in hepatic tissues. (A) Level of *p53* mRNA in hepatic tissues. (B) Level of *Bcl-2* mRNA in hepatic tissues. (C) Level of *Bcl-xL* mRNA in hepatic tissues. n=8 per group. *P<0.05 vs. control; #P<0.05 vs. model. BL, berberine low-dose; BM, berberine middle-dose; BH, berberine high-dose; PC, positive control.
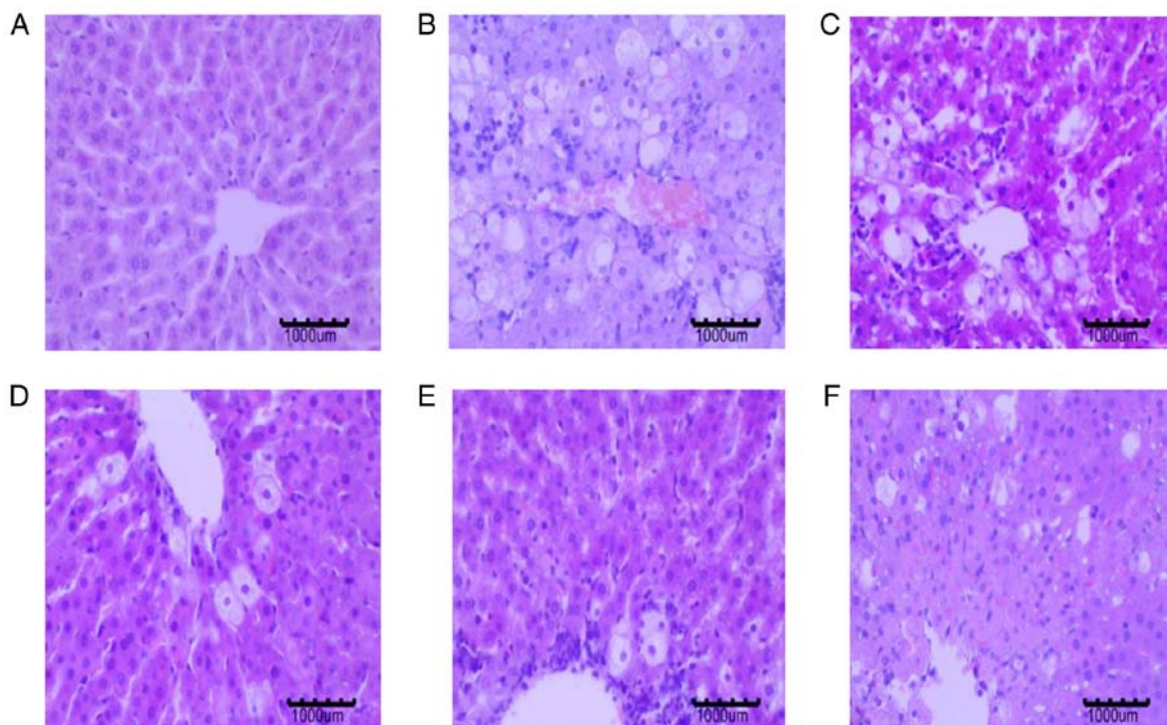

Figure 7. Liver pathological changes in rats. (A) Liver pathology of the control group. (B) Liver pathology of the model group. (C) Liver pathology of the BBR low-dose group. (D) Liver pathology of the BBR middle-dose group. (E) Liver pathology of the BBR high-dose group. (F) Liver pathology of the positive control group. n=8 per group. Magnification, x400. BBR, berberine.

the BBR-treated and PC groups, and necrotic hepatocytes and fatty degeneration of hepatocytes was significantly reduced (Fig. 7).

Effects of BBR on HO-1 protein. The western blotting results showed a decrease in the expression of HO-1 in the model group compared with the control group, and that in the BBR-treated
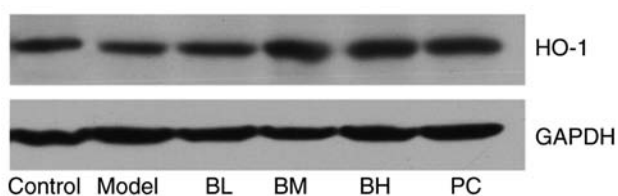
Figure 8. Expression of HO-1 protein in livers of rats in each group. n=8 per group. HO-1, heme oxygenase 1; BL, berberine low-dose; BM, berberine middle-dose; BH, berberine high-dose; PC, positive control.

and PC groups was increased when compared with the model group (Fig. 8).

Discussion

The liver is the main organ involved in the metabolism of drugs and toxic chemicals of the human body and is highly susceptible to damage caused by drugs, poisons and viruses. The ALI model generated by CCl_4 treatment is widely used in the study of chemical liver injury and hepatoprotective screening (9,10). The mechanism of ALI induced by CCl_4 is complex. Oxidative stress, lipid peroxidation, changes in the activity and content of metabolic enzymes, cytokines, apoptosis, and many other factors are involved in this process (11-13); oxidative stress is considered to be the main pathogenetic process of liver injury induced by CCl_4. Oxidative stress means that when stimulated by certain harmful factors, the body will produce excessive high-activity molecules, such as ROS and reactive nitrogen species, resulting in an imbalance between the oxidation and antioxidant defense systems. Neutrophil inflammatory infiltration occurs, and a large number of oxidative intermediates are produced, causing tissue cell damage (14). When hepatocytes are damaged, cell membrane permeability will increase and cytoplasmic transaminases, such as ALT and AST, can be released into the blood in large amounts (15,16). MDA, the product of membrane lipid peroxidation, can exacerbate cell membrane damage. When CCl_4 induces lipid peroxidation damage in the liver, HO-1, GSH peroxidase, SOD and GSH are reduced to varying degrees (17).

Serum aminotransferases ALT, AST and ALP are the most effective indicators of early liver injury (18). When hepatocytes are damaged, ALT and AST are released in large amounts into the blood, and serum ALT and AST levels are increased. In this experiment, the levels of serum ALT, AST and ALP in the model group were significantly increased. After treatment with BBR, the levels of serum ALT, AST and ALP were significantly decreased, indicating that BBR can alleviate CCl_4-induced ALI to a certain extent, consistent with the histopathological results.

SOD and GSH are important antioxidant enzymes in the body, which can effectively eliminate free radicals and inhibit free radical-induced lipid peroxidation (19). As the final metabolite of lipid peroxidation, the MDA level reflects the degree of oxidative stress caused by toxophores (20). Liu et al (10) showed that CCl_4 could disrupt the antioxidant system, reduce the levels of GSH and SOD, and raise the level of MDA, promoting further development of liver damage. The results of the current study showed that BBR could ameliorate

CCl_4-induced liver injury by increasing T-SOD and GSH levels and reducing MDA, indicating that the hepatoprotective effects of BBR may be related to antioxidative stress.

The Nrf2-ARE signaling pathway is a key pathway for cellular antioxidant stress, and the antioxidant enzyme system and phase II detoxification enzymes regulated by this signaling pathway can eliminate harmful substances, such as ROS (21,22). The activated Nrf2-ARE signaling pathway can induce the transcription of protective genes, such as HO-1, glutathione-S-transferase and NQO1, to resist oxidative stress damage caused by various stimulating factors (23). Hsu et al (24) demonstrated that BBR could promote the nuclear translocation of Nrf2 in motor neuron-like cell lines. According to Chen et al (25), BBR can upregulate the transcription of the HO-1 gene in primary astrocytes. Additionally, Zhang et al (26) reported that BBR further activates Nrf2 by activating the AMPK pathway, PI3K/Akt pathway and the p38 pathway, increasing the expression of HO-1 and SOD, reducing ROS production, and, in turn, attenuating oxidative stress. The results presented herein showed that BBR could significantly reduce the level of ROS in the body and upregulate the expression of Nrf2, Keap-1, NQO-1 and HO-1 in cells, further indicating that the hepatoprotective effect of BBR is related to antioxidative stress.

When DNA damage occurs, or the cells are stimulated by ROS, the tumor suppressor p53 may be involved in the regulation of apoptosis. p53 promotes apoptosis by upregulating the pro-apoptotic gene Bax and downregulating the expression of anti-apoptotic genes Bcl-2 and Bcl-xL (27,28). Tiwari et al (29) revealed that HO-1 produced by oxidative stress could inhibit apoptosis by upregulating the expression of Bcl-2 and Bcl-xL proteins. Sha et al (30) indicated that BBR hydrochloride could induce apoptosis in human gastric cancer cells, and its mechanism may be closely related to the upregulation of Bax and p53 protein, and downregulation of Bcl-2 protein.

The results of the present study showed that BBR could significantly reduce the expression of p53 mRNA, and increase the expression of Bcl-2 and Bcl-xL mRNA, to different extents. BBR effectively protects against CCl_4-induced ALI in rats, and its mechanism may inhibit ROS production, reduce serum ALT, AST and ALP levels, and increase T-SOD, GSH and MDA. BBR activates the Nrf2-Keap1-ARE signaling pathway, to regulate the expression of Nrf2, Keap-1, NQO-1 and HO-1 genes, and inhibits hepatocyte apoptosis by downregulating the p53 gene and upregulating the Bcl-xL and Bcl-2 genes.

One limitation of the present study was the lack of TUNEL staining to detect the level of apoptosis before and after treatment with BBR. Future studies will use TUNEL staining to assess apoptosis. Further in vitro experiments are required to elucidate the upstream and downstream pathways of Nrf2-Keap1-ARE.

China (grant no. KJ2017A129); and The National Natural Science Foundation of China (grant no. 31172358).

Authors' contributions

CYH, JGG and CYL contributed to the design of the experiment. CYH, TTS and GPX performed all experiments and verified the analytical data. SSW and TTS contributed to the statistical analysis and helped interpret the results. CYH and CYL wrote the manuscript. All authors discussed the final results and approved the final manuscript.

Ethics approval and consent to participate

All procedures were in strict accordance with the Chinese legislation on the use and care of laboratory animals and the guidelines established by the Institute for Experimental Animals of Anhui Agriculture University, and were approved by the Anhui Agriculture University Committee on Animal Care and Use.

Patient consent for publication

Not applicable.

Competing interests

The authors declare that they have no competing interests.

References

1. Shin DS, Kim KW, Chung HY, Yoon S and Moon JO: Effect of sinapic acid against carbon tetrachloride-induced acute hepatic injury in rats. Arch Pharm Res 36: 626-633, 2013.
2. Imanshahidi M and Hosseinzadeh H: Pharmacological and therapeutic effects of Berberis vulgaris and its active constituent, berberine. Phytother Res 22: 999-1012, 2008.
3. Jiang Q, Liu P, Wu X, Liu W, Shen X, Lan T, Xu S, Peng J, Xie X and Huang H: Berberine attenuates lipopolysaccharide-induced extracelluar matrix accumulation and inflammation in rat mesangial cells: Involvement of NF-κB signaling pathway. Mol Cell Endocrinol 331: 34-40, 2011.
4. Hasanein P, Ghafari-Vahed M and Khodadadi I: Effects of isoquinoline alkaloid berberine on lipid peroxidation, antioxidant defense system, and liver damage induced by lead acetate in rats. Redox Rep 22: 42-50, 2017.
5. Liu RY and Chen CT: In vitro antibacterial activity assay of 8 herbs (including *Coptis chinensis*) on several conditional pathogenic bacteria that often cause nosocomial infection. J Fujian Univ Tradit Chin Med 14: 26-28, 2004 (In Chinese).
6. Chen FL, Yang ZH, Liu Y, Li LX, Liang WC, Wang XC, Zhou WB, Yang YH and Hu RM: Berberine inhibits the expression of TNFalpha, MCP-1, and IL-6 in AcLDL-stimulated macrophages through PPARgamma pathway. Endocrine 33: 331-337, 2008.
7. Gu M, Xu J, Han C, Kang Y, Liu T, He Y, Huang Y and Lic C: Effects of Berberine on cell cycle, DNA, reactive oxygen species and apoptosis in L929 murine fibroblast cells. Evid Based Complement Alternat Med 2015: 796306, 2015.
8. Livak KJ and Schmittgen TD: Analysis of relative gene expression data using real-time quantitative PCR and the 2(-Delta Delta C(T)) method. Methods 25: 402-408, 2001.
9. Chang ML, Yeh CT, Chang PY and Chen JC: Comparison of murine cirrhosis models induced by hepatotoxin administration and common bile duct ligation. World J Gastroenterol 11: 4167-4172, 2005.
10. Liu Y, Zheng D, Su L, Wang Q and Li Y: Protective effect of polysaccharide from Agaricus bisporus in Tibet area of China against tetrachloride-induced acute liver injury in mice. Int J Biol Macromol 118: 1488-1493, 2018.
11. Wang YZ: The protective effect of polysaccharide of *Grifola frondosa* on carbon tetrachloride-induced liver injury and its mechanism. Shandong Univ, 2010.
12. Dong D, Zhang S, Yin L, Tang X, Xu Y, Han X, Qi Y and Peng J: Protective effects of the total saponins from *Rosa laevigata* Michx fruit against carbon tetrachloride-induced acute liver injury in mice. Food Chem Toxicol 62: 120-130, 2013.
13. Huang QX: Relationship between hepatic stellate cells and inflammation. Internal Med 2: 978-979, 2007.
14. Zhang HY, Li XW, Yao XL and Zhu JX: Progress in molecular mechanism and traditional chinese medicine pharmacology for liver injury. Tradit Chin Drug Res Clin Pharmacol 27: 448-455, 2016 (In Chinese).
15. Lee CH, Park SW, Kim YS, Kang SS, Kim JA, Lee SH and Lee SM: Protective mechanism of glycyrrhizin on acute liver injury induced by carbon tetrachloride in mice. Biol Pharm Bull 30: 1898-1904, 2007.
16. Gan D, Ma L, Jiang C, Wang M and Zeng X: An international journal published for the british industrial biological research association. Food Chem Toxicol 50: 2681-2688, 2012.
17. Liu LP, Tao XF, Han X and Xu L: Research progress in the inhibitory effect of traditional chinese medicine on carbon tetrachloride induced acute liver injury. China Pharmacist 20: 1638-1642, 2017.
18. Stadler RH, Blank I, Varga N, Robert F, Hau J, Guy PA, Robert MC and Riediker S: Acrylamide from maillard reaction products. Nature 419: 449-450, 2002.
19. Radu CD, Salariu M, Avadanei M, Ghiciuc C, Foia L and Elena CL: Carbohydrate Polymers. 1981.
20. Suji G and Sivakami S: Malondialdehyde, a lipid-derived aldehyde alters the reactivity of Cys34 and the esterase activity of serum albumin. Toxicol In Vitro 22: 618-624, 2008.
21. Kundu JK and Surh YJ: Nrf2-Keap1 signaling as a potential target for chemoprevention of inflammation-associated carcinogenesis. Pharm Res 27: 999-1013, 2010.
22. Hou Y, Wang Y, He Q, Li L, Xie H, Zhao Y and Zhao J: Nrf2 inhibits NLRP3 inflammasome activation through regulating Trx1/TXNIP complex in cerebral ischemia reperfusion injury. Behav Brain Res 336: 32-39, 2018.
23. Li L, Dong H, Song E, Xu X, Liu L and Song Y: Nrf2/ARE pathway activation, HO-1 and NQO1 induction by polychlorinated biphenyl quinone is associated with reactive oxygen species and PI3K/AKT signaling. Chem Biol Interact 209: 56-67, 2014.
24. Hsu YY, Chen CS, Wu SN, Jong YJ and Lo YC: Berberine activates Nrf2 nuclear translocation and protects against oxidative damage via a phosphatidylinositol 3-kinase/Akt-dependent mechanism in NSC34 motor neuron-like cells. Eur J Pharm Sci 46: 415-425, 2012.
25. Chen JH, Huang SM, Tan TW, Lin HY, Chen PY, Yeh WL, Chou SC, Tsai CF, Wei IH and Lu DY: Berberine induces heme oxygenase-1 up-regulation through phosphatidylinositol 3-kinase/AKT and NF-E2-related factor-2 signaling pathway in astrocytes. Int Immunopharmacol 12: 94-100, 2012.
26. Zhang C, Li C, Chen S, Li Z, Jia X, Wang K, Bao J, Liang Y, Wang X, Chen M, *et al*: Berberine protects against 6-OHDA-induced neurotoxicity in PC12 cells and zebrafish through hormetic mechanisms involving PI3K/AKT/Bcl-2 and Nrf2/HO-1 pathways. Redox Biol 11: 1-11, 2017.
27. Kuwana T, Mackey MR, Perkins G, Ellisman MH, Latterich M, Schneiter R, Green DR and Newmeyer DD: Bid, Bax, and lipids cooperate to form supramolecular openings in the outer mitochondrial membrane. Cell 111: 331-342, 2002.
28. Baek JH, Jang JE, Kang CM, Chung HY, Kim ND and Kim KW: Hypoxia-induced VEGF enhances tumor survivability via suppression of serum deprivation-induced apoptosis. Oncogene 19: 4621-4631, 2000.
29. Tiwari M, Tripathi A and Chaube SK: Presence of encircling granulosa cells protects against oxidative stress-induced apoptosis in rat eggs cultured in vitro. Apoptosis 22: 98-107, 2017.
30. Sha SM, Zhang YG, Xu B, Wang HL, Kong XY and Wu KC: Effect of Berberine on cell proliferation and apoptosis in gastric carcinoma cells. J Mod Oncol 19: 629-633, 2011.